Initial Rotor Position Estimation of a Surface Mounted PMSM

Ying Yan, Jianguo Zhu, Greg Hunter, and Youguang Guo
Faculty of Engineering, University of Technology, Sydney, PO Box 123, Broadway, NSW 2007, Australia

***Abstract*—The direct torque controlled (DTC) permanent magnet synchronous motor (PMSM) has become attractive because of its simplicity and fast torque response. However, mechanical position sensors have caused problems. It is possible to eliminate mechanical position sensors if the initial rotor position is known. In order to start the system under full load, a method to identify the initial rotor position is necessary. This paper presents a nonlinear model incorporating both the structural and saturation saliencies to enable the numerical simulation of new rotor position detection algorithms, which is applicable for surface mounted PMSMs. In this model, the winding inductances are expressed as the functions of stator currents and rotor position. A scheme for initial rotor position estimation is investigated. Based on the presented model, simulation by this scheme is conducted. Experiments are carried out and the results are compared with the simulation results to verify the effectiveness of the model.**

***Index Terms*—Initial rotor position estimation, surface mounted PMSM.**

I. Introduction

Sensorless control of permanent magnet synchronous motors (PMSMs) has become very attractive because of its many advantages over the systems with mechanical position and/or speed sensors, such as significant reduction of system hardware complexity and increase of the system reliability. A great amount of research has been conducted on position sensorless techniques and various methods have been proposed by different researchers. Among them, the most versatile is to detect the structural and/or magnetic saturation saliencies of the PMSM [1-2].

Generally, there are two types of saliencies within an electric machine: structural saliency and magnetic saturation saliency. For the electric machines with large structural saliency, e.g. interior type PMSM, the structural saliency-based rotor position identification can be very effective. The magnetic saturation saliency is caused by the saturation of magnetic core. In a PMSM, this kind of saliency is mainly caused by the permanent magnets (PMs) on the rotor, although it is also affected by the magnetic field produced by the stator current. In a surface mounted PMSM (SPMSM) with small structural saliency, the saturation saliency may have to be used.

Since the conventional PMSM model does not incorporate the saturation saliency, when developing a new method for the initial rotor position detection, it is not possible to numerically simulate the method, and the experimental trial and error method is widely used. In this paper, a nonlinear PMSM model which incorporates both the structural and saturation saliencies is derived. In this model, the saliencies of the motor are reflected by the variation of the stator winding inductances with respect to the rotor positions and stator currents. The analytical expression of the incremental inductances is established based on the measurement of an SPMSM and Fourier series. A scheme for initial rotor position detection is investigated. Based on the presented model, simulation by the scheme is conducted and the results are compared with the experimental results to verify the effectiveness of the model.

II. Nonlinear Model of PMSM

In a PMSM, the field produced by the rotor magnets is the dominant component. Although the characteristics of the magnetic core is nonlinear, the magnetic circuit can be considered as piecewisely linearized around the operating point P at a given rotor position. Thus, the total flux linkage of phase a, ψ_a, can be separated into two components [3-5].

$$\psi_a = \psi_{as}\left(i_{ms}, \theta\right) + \psi_{af} \tag{1}$$

where θ is the rotor position, and ψ_{as} and ψ_{af} are the flux linkage components produced by the magnetization component of the stator current i_{ms}, and rotor magnets, respectively. The flux linkage ψ_{as} can be further separated into components attributed by individual stator phase currents, ψ_{aa}, ψ_{ab}, and ψ_{ac}.

$$\psi_a = \psi_{aa} + \psi_{ab} + \psi_{ac} + \psi_{af} \tag{2}$$

where ψ_{aa}, ψ_{ab}, and ψ_{ac} are the flux linkage components of phase a corresponding to each phase current. Under the assumption of linearization, the flux linkage components, ψ_{aa}, ψ_{ab}, and ψ_{ac} can be considered as proportional to the corresponding phase currents: $\psi_{aa}=L_{aa}(i_a, \theta)i_a$, $\psi_{ab}=L_{ab}(i_b, \theta)i_b$, $\psi_{ac}=L_{ac}(i_c, \theta)i_c$.

The proportionality coefficients L_{aa}, L_{ab}, and L_{ac}, which are determined by the gradient of the magnetization curve at the operating point, are defined as the self and mutual incremental inductances of the phase a winding. The flux linkages of phases b and c can be obtained similarly. The voltage equations of the three-phase stator windings can be written as:

$$\begin{bmatrix} v_a \\ v_b \\ v_c \end{bmatrix} = \begin{bmatrix} R_a & 0 & 0 \\ 0 & R_b & 0 \\ 0 & 0 & R_c \end{bmatrix} \begin{bmatrix} i_a \\ i_b \\ i_c \end{bmatrix} + \left[L_T\right] \frac{d}{dt} \begin{bmatrix} i_a \\ i_b \\ i_c \end{bmatrix} + \begin{bmatrix} e_{af} + e_{a\theta} \\ e_{bf} + e_{b\theta} \\ e_{cf} + e_{c\theta} \end{bmatrix} \tag{3}$$

where

$$[L_T]=\begin{bmatrix} L_{aa}+i_a\dfrac{\partial L_{aa}}{\partial i_a} & L_{ab}+i_b\dfrac{\partial L_{ab}}{\partial i_b} & L_{ac}+i_c\dfrac{\partial L_{ac}}{\partial i_c} \\ L_{ab}+i_a\dfrac{\partial L_{ab}}{\partial i_a} & L_{bb}+i_b\dfrac{\partial L_{bb}}{\partial i_b} & L_{bc}+i_c\dfrac{\partial L_{bc}}{\partial i_c} \\ L_{ac}+i_a\dfrac{\partial L_{ac}}{\partial i_a} & L_{bc}+i_b\dfrac{\partial L_{bc}}{\partial i_b} & L_{cc}+i_c\dfrac{\partial L_{cc}}{\partial i_c} \end{bmatrix}$$

v_a, v_b, and v_c are the terminal voltages, R_a, R_b, and R_c the winding resistances, i_a, i_b, and i_c the currents of phases *a*, *b*, and *c*, respectively, $e_{af}=\omega_r d\psi_{af}/d\theta$, $e_{bf}=\omega_r d\psi_{bf}/d\theta$, and $e_{cf}=\omega_r d\psi_{cf}/d\theta$ the electromotive forces (*emfs*) induced by the rotor magnets, and $\omega_r=d\theta/dt$ is the mechanical angular speed of the rotor. $e_{a\theta} = \omega_r(i_a\partial L_{aa}/\partial\theta+ i_b\partial L_{ab}/\partial\theta+i_c\partial L_{ac}/\partial\theta)$, $e_{b\theta} = \omega_r(i_a\partial L_{ab}/\partial\theta+ i_b\partial L_{bb}/\partial\theta+ i_c\partial L_{bc}/\partial\theta)$, and $e_{c\theta} = \omega_r(i_a\partial L_{ac}/\partial\theta+ i_b\partial L_{bc}/\partial\theta+ i_c\partial L_{cc}/\partial\theta)$ are the three phase *emfs* induced by the variation of flux linkage due to the saliencies.

The electromagnetic torque of the PMSM can be obtained by taking the partial derivative of the system magnetic co-energy, W_f', with respect to the rotor position angle θ, i.e. $T=\partial W_f'/\partial\theta$, and it can be derived as:

$$T=\frac{\partial\psi_{af}}{\partial\theta}i_a+\frac{\partial\psi_{bf}}{\partial\theta}i_b+\frac{\partial\psi_{cf}}{\partial\theta}i_c+\frac{\partial L_{aa}}{\partial\theta}\frac{i_a^2}{2}+\frac{\partial L_{bb}}{\partial\theta}\frac{i_b^2}{2}+\frac{\partial L_{cc}}{\partial\theta}\frac{i_c^2}{2}+\frac{2\partial L_{ab}}{\partial\theta}i_ai_b+\frac{2\partial L_{ac}}{\partial\theta}i_ai_c+\frac{2\partial L_{bc}}{\partial\theta}i_bi_c \quad (4)$$

The electromagnetic torque has two components: one produced by the stator currents and rotor magnets, and the other by the saliencies.

III. Nonlinear Incremental Inductance

A. Analytical Expression of Nonlinear Inductance

As discussed above, the self and mutual inductances of the stator windings with structural and magnetic saturation saliencies are the nonlinear functions of the stator currents and rotor position, which require a large amount of data to describe numerically. The incorporation of the analytical expressions of these inductances could simplify the implementation of the numerical simulation model and reduce significantly the amount of parameters.

The relationship between the phase inductance and the rotor position can be expressed by a Fourier series [6]. The different sets of coefficients of the Fourier series, a_0, a_m, and b_m ($m=1, 2, \ldots, n$), can be obtained with different currents, and expressed as the functions of the corresponding currents. Therefore, we have:

$$L(i,\theta)=a_0(i)+\sum_{m=1}^{n}\left(a_m(i)\cos m\theta+b_m(i)\sin m\theta\right) \quad (5)$$

For a group of measured phase inductances, $L(\theta_j,i_k)$, the coefficients of the corresponding Fourier series can be obtained by nonlinear curve fitting, where *j* and *k* refer to the various experimental rotor positions and currents, respectively. The nonlinear model of the self and mutual inductances can be readily incorporated into the PMSM model presented in Section II.

B. Experimental Measurement of Phase Inductances

In its normal operating state, the total flux linkage of a PMSM is composed of the flux produced by the rotor PMs and stator currents, or $\psi_t = \psi_r+\psi_s$, and hence, the phase inductances are related to both of them. In order to estimate the saturation effect at various stator fluxes, DC offsets, i_{dc}, are used to emulate the effect of the three-phase currents. A method for measuring the phase inductances is designed to express the relationship between the inductance variation and the saturation of magnetic core.

The experiment is carried out on a 6-pole surface mounted PMSM, and the rotor of the motor is locked by a dividing head. Various DC offsets are injected to one of the stator windings. Meanwhile, a small AC current is applied to one phase while the other two are open-circuited. With this method, the self and mutual inductances of phases *a*, *b* and *c* at different rotor positions and stator currents can then be obtained.

It can be concluded that the inductances are the functions of amplitudes and angles of both stator and rotor fluxes, $L(\theta_s,\theta_r,|\Phi_s|,|\Phi_r|)$, where θ_s is the position of the stator rotating flux, θ_r the position of rotor flux, and $|\Phi_s|$ and $|\Phi_r|$ are the amplitudes of the stator and rotor fluxes, respectively. Since the amplitude of the rotor flux produced by the PMs can be considered as a constant, the inductances can be simplified as functions of θ_s, θ_r, and $|\Phi_s|$, and rewritten as $L(\theta_s,\theta_r,|\Phi_s|)$.

In order to simplify the inductance expressions, the angle between the stator flux, Φ_s, and the stator winding axis of phase *a*, denoted by α, and the angle between the stator and rotor fluxes, denoted by δ, as shown in Fig. 1, are used in the inductance model instead of θ_s and θ_r. The phase *a* inductance, $L_{sa}(\alpha, \delta, i_{ms})$, at any stator and rotor fluxes ($\alpha=0°\sim360°$, $\delta=0°\sim360°$, and $i_{ms}=0\sim I_{rated}$) can be estimated by linear interpolation of the inductance expression measured by injecting various DC currents to phase *a* at $\alpha=0°$, $\alpha=120°$, and $\alpha=240°$ with $\delta=0°\sim360°$, and $i_{ms}=0\sim I_{rated}$. Due to the symmetry of the three phase windings, the inductances of phases *b* and *c* at any rotor position and stator current can be estimated based on the phase *a* inductance expression by shifting the rotor position by $\pm120°$, respectively. Similar procedure can be applied to estimate the mutual inductances. Therefore, the structural and saturation saliencies of the motor magnetic filed could be mapped out in terms of the three phase self and mutual inductances. Figs. 2 and 3 illustrate L_{sa} and L_{mab}, at different rotor positions with a DC offset of 5.5A applied to different α.

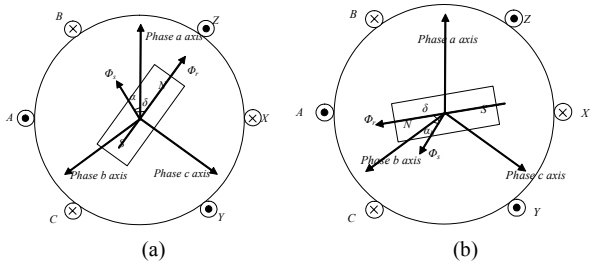

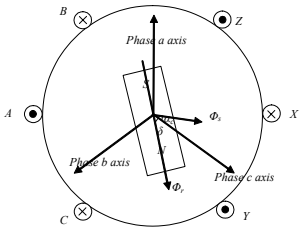

(c)

Fig. 1. (a) Rotor and stator fluxes linking phase *a* with a DC offset in phase *a*; (b) Rotor and stator fluxes linking phase *b* with a DC offset in phase *a*; (c) Rotor and stator fluxes linking phase *c* with a DC offset in phase *a*.

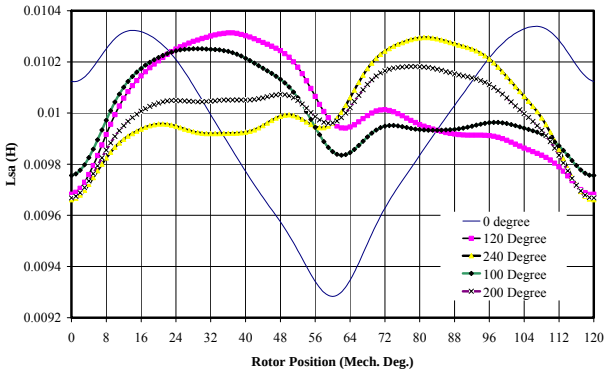

Fig. 2. Measured and calculated L_{sa} at different α.

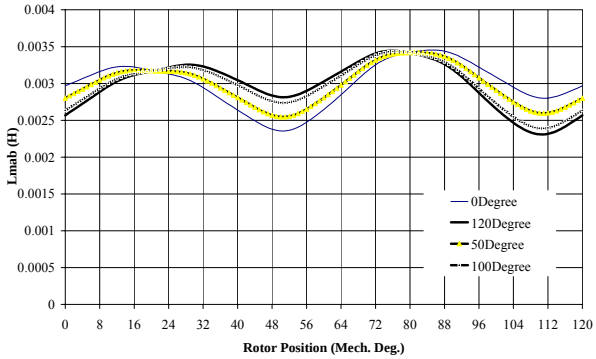

Fig. 3. Measured and calculated L_{mab} at different α.

IV. Estimation of Initial Rotor Position

A. Schemes for Initial Rotor Position Estimation

In the DTC scheme, the starting procedure under full load is very difficult because no current or *emf* information is available for determining the rotor position before starting. Therefore, it is essential to develop a sensorless method to determine the initial rotor position for full load starting of PMSM drive systems. Numerous approaches have been proposed to estimate the initial rotor position based on the parameters from the motor's terminals. Most of them are effective for the motor with large structural saliency, e.g. the interior PMSM. However, in a surface mounted PMSM, it becomes difficult due to the small saliencies. The saturation saliency may have to be used because the structural saliency is not significant.

It has been discussed that the winding inductance is a function of rotor position and stator current. With this feature, the initial rotor position can be estimated by injecting voltage pulses with high amplitude, as shown in Fig. 4, to the stator winding terminals [7-8]. At an unknown initial rotor position, one of the three phase terminals, say phase *a*, is applied with a positive pulse while the terminals of the other two phases are applied with a negative pulse. After a certain time interval, the positive pulse is followed by a negative pulse and the negative pulse by a positive pulse to bring down the currents in the phase windings to zero.

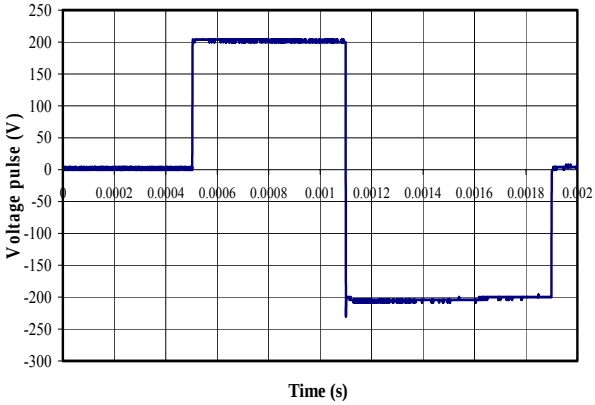

Fig. 4. High voltage pulse.

B. Experimental Results

Experiment with the above scheme is carried out. In the experiment, the high voltage pulse is applied to the testing SPMSM through a PWM inverter, and the gate signals of the inverters are controlled by a dSPACE DS1104 system. For example, when the positive pulse is applied to phase *a*, the gate signals of 100 are created and applied to the inverter, and the equivalent circuit is shown in Fig. 5. The corresponding phase currents are measured by current probes and an oscilloscope. Fig. 6 depicts the three phase current response recorded for high voltage pulses with gate signals 100, 010 and 001, respectively. For each phase, the measurement is taken at every locked rotor position and the motor is mechanically rotated from one position to the next. The measured three phase peak currents at different rotor positions with high voltage pulses are plotted in Figs. 7.

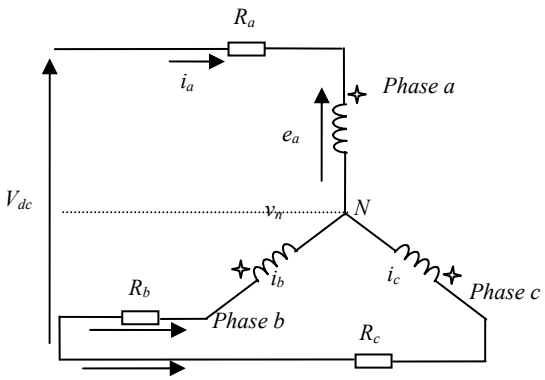

Fig. 5. Equivalent circuit of the motor at standstill.

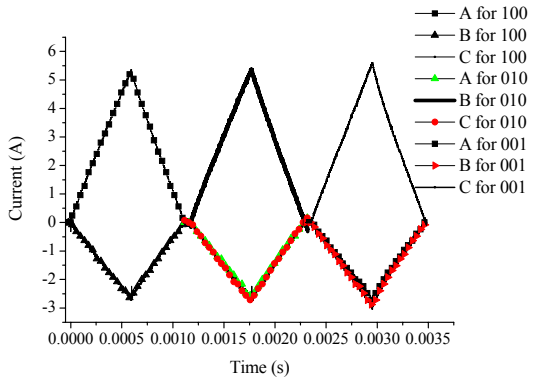

Fig. 6. Experimental current response to high voltage pulse.

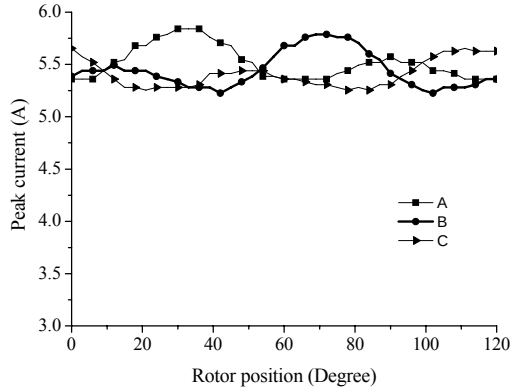

Fig. 7. Peak current versus rotor position with high voltage pulse.

C. Comparison of Simulated and Measured Peak Currents

Based on the equivalent circuit of a PMSM at standstill, a Simulink model is built and the voltage pulse injection algorithm outlined above is numerically simulated with the measured inductances as the parameters. Fig. 8 plots both the simulated and measured peak currents of phase *a*, *b* and *c* versus the rotor position when a high voltage pulse of 200 V in magnitude and 0.6 ms pulse width is applied. As shown in Fig. 6, the general profiles of the simulated and experimental peak currents are similar. As mentioned previously, the self and mutual inductances were measured only at limited rotor positions with DC offsets applied only in phase *a* winding, and the linear interpolation is performed to deduce the inductances at other rotor and DC offset field positions. This means the inductance values at these positions may be inaccurate and therefore, some error would appear in the simulated results at those specific positions.

D. Comparison of Peak Current and Inductance Variation

Compared with the almost sinusoidal waveform under the non-saturated condition, it can be seen that with the high voltage pulse, the magnetic saturation becomes evident.

As shown in Fig. 9, for the SPMSM, the positions of the *d*- and *q*-axes can be clearly identified from both profiles of the inductance measured with and without the DC offset because the *q*-axis inductance is higher than the *d*-axis inductance, while only the inductance profile with DC offset can reveal the rotor polarity (north or south pole). Due to the structural saliency, the stator current produced by the high voltage pulse reaches a valley when the magnetic field of the stator current is on the *q*-axis, and a peak when the stator field is on the *d*-axis.

Once the position of the *d*-axis is determined, the rotor polarity can be determined by comparing the magnitudes of the stator currents on the *d*-axis. If the stator field aids the rotor field (same polarity) on the *d*-axis, the magnetic circuit becomes more saturated, and thus the magnitude of the stator current would be higher than that when the stator field opposes the rotor field (opposite polarity) and the magnetic circuit becomes less saturated [7]. Therefore, detection of the initial rotor position by means of the structural and saturation saliencies is feasible.

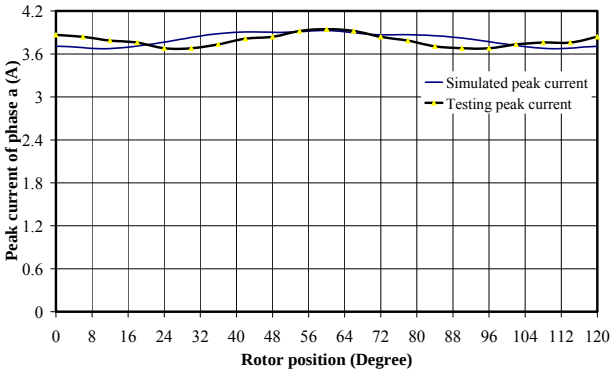

(a)

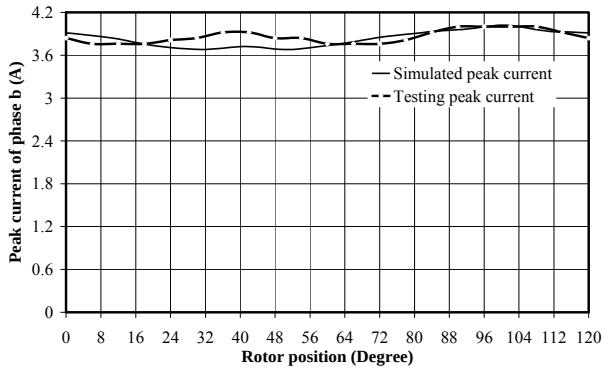

(b)

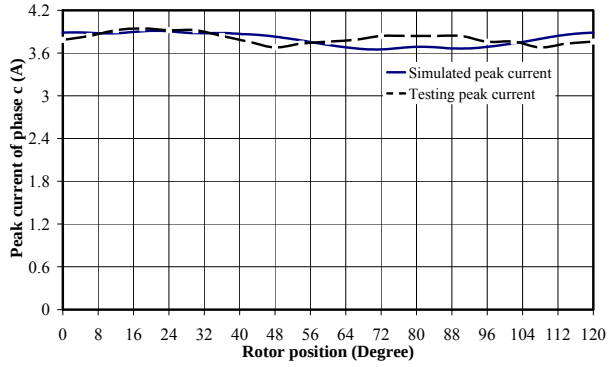

(c)

Fig. 8. Comparison of simulated and measured peak currents of (a) phase *a*, (b) phase *b*, and (c) phase *c*.

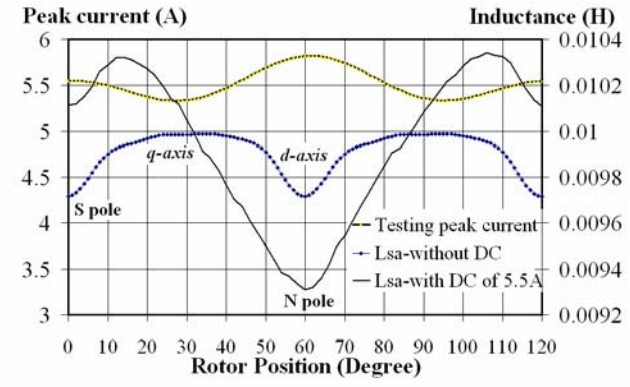

(a)

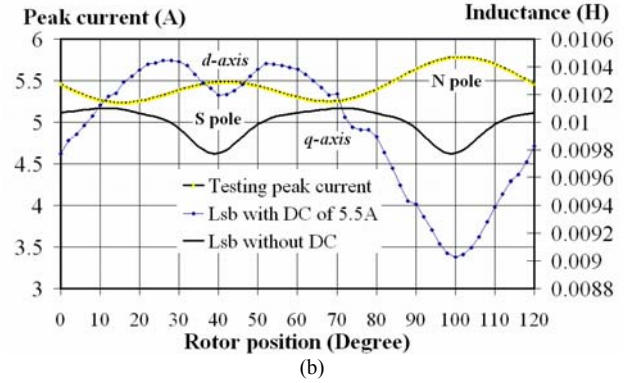

(b)

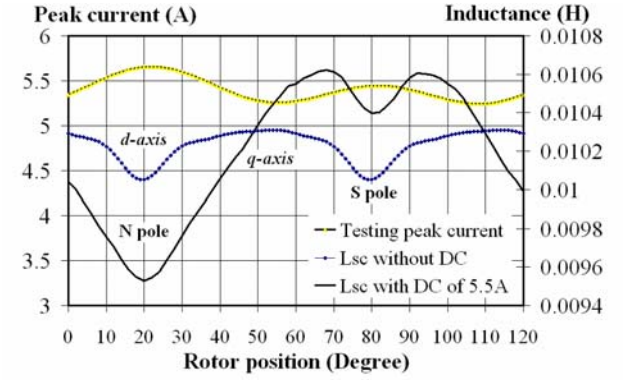

(c)

Fig. 9. Inductance and peak current variation of (a) Phase *a*, (b) Phase *b*, (c) Phase *c*.

E. An Algorithm for Detecting Initial Rotor Position

The above analysis shows that it is quite feasible to identify the positions of the *d*- and *q*-axes and the rotor polarity from the measured peak current versus rotor position curve. The phase currents shown in Fig. 7 can be modeled by an average value, I_0, plus some offset values, ΔI_{01} and ΔI_{02}, as a function of rotor position, θ, as the following:

$$I_a = I_0 + I_{01}\cos(\theta) + I_{02}\cos(2\theta) \tag{6}$$

$$I_b = I_0 + I_{01}\cos\left(\theta - \frac{2\pi}{3}\right) + I_{02}\cos\left(2\theta + \frac{2\pi}{3}\right) \tag{7}$$

$$I_c = I_0 + I_{01}\cos\left(\theta + \frac{2\pi}{3}\right) + I_{02}\cos\left(2\theta - \frac{2\pi}{3}\right) \tag{8}$$

where I_a, I_b and I_c are peak currents and θ rotor position, I_0, ΔI_{01} and ΔI_{02} can be obtained by curve fitting the experimental results as shown in Fig. 7. Fig. 10 plots the curve fitting results of the experimental data.

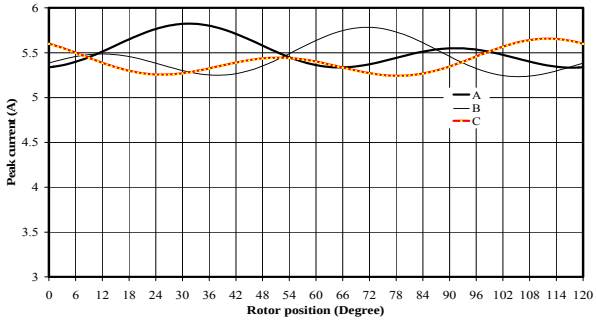

Fig. 10. Fitted peak current with high voltage pulses.

Based on the above analysis, a simple algorithm is composed for detecting the initial rotor position. The measured peak current curves of phases *a*, *b* and *c* at different rotor positions are stored in the memory of the microprocessor in the form of a look up table. When the rotor is standstill, send 100, 010, and 001 gate signals to the PWM inverter to apply high voltage pulses to the three phase stator winding terminals, and record the peak phase currents. Possible rotor positions can be readily found by solving inversely (6), (7), and (8) using a sectional interpolation method. For phase *a*, the possible rotor positions corresponding to the peak current I_{ap} can be obtained as θ_{a1} θ_{a2}, θ_{a3} and so on, and similarly, for phases *b* and *c*, the possible rotor positions corresponding to I_{bp} and I_{cp} can be obtained as θ_{b1} θ_{b2}, θ_{b3}, θ_{c1} θ_{c2}, θ_{c3} and so on. Among all these possible rotor positions, the real rotor position is given by the common angle obtained of all the three phases.

Experiment is carried out to verify the validity of the algorithm. The estimated electrical rotor angle that was obtained with the above algorithm was plotted as a function of the actual mechanical rotor angle and is shown in Fig. 11. The actual rotor angle was measured using an optical encoder attached to the motor shaft and the dividing head used to fix the rotor. It can be seen that this algorithm can produce satisfactory results.

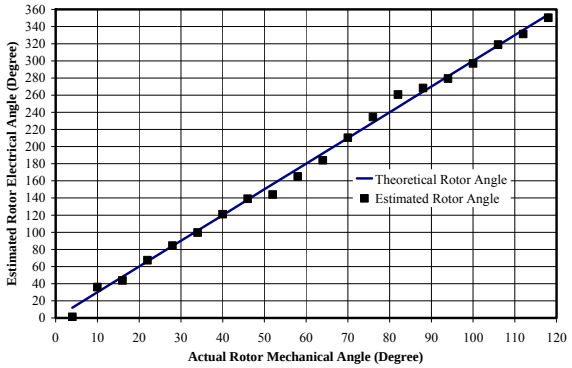

Fig. 11. Estimated rotor electrical angle versus actual rotor mechanical angle.

V. CONCLUSIONS

A nonlinear PMSM model incorporating both the structural and magnetic saturation saliencies has been presented in this paper. In the model, the saliencies are reflected by the variation of the stator winding inductances with respect to the rotor position and stator phase currents. The nonlinear inductances of a surface mounted PMSM at various rotor positions and stator currents are experimentally measured and discussed. The Fourier series are employed to express the inductances as the functions of rotor position and stator currents. The small structural saliency in the surface mounted PMSM is revealed in the self and mutual inductance profiles versus rotor position without any DC offset, but when DC offset currents are applied in the stator phase windings, the effect of magnetic saturation becomes evident.

The schemes for detecting the initial rotor position by injecting high voltage pulse are investigated by both numerical simulation and experimental testing. Corresponding to the high voltage pulses, the peak stator currents are strong enough to produce reasonably large magnetic saturation saliency for identifying the rotor position and polarity. A simple numerical algorithm for detecting the initial rotor position from the peak stator current variation is proposed. The validity and accuracy of this algorithm is confirmed by a numerical simulation before it is implemented in real time system. The effectiveness of this algorithm is also verified by the experimental results.

REFERENCES

[1] P.L. Jansen and R.D. Lorenz, "Transducerless position and velocity estimation in induction and salient AC machines," *Conference Record of IEEE IAS Annual Meeting*, Oct. 1994, vol. 1, pp. 488-495.

[2] S. Ogasawara and H. Akagi, "Implementation and position control performance of a position-sensorless IPM motor drive system based on magnetic saliency," *Conference Record of the Thirty-Second IEEE IAS Annual Meeting*, Oct. 5-9, 1997, vol.1, pp. 464-470.

[3] Y. Yan, J.G. Zhu, H.W. Lu, Y.G. Guo, and S.H. Wang, "A PMSM Model Incorporating Structural and Saturation Saliencies," *Proc. of 8th Int. Conf. on Electrical Machines and Systems*, Nanjing, China, Sept. 2005, pp. 194-199.

[4] Y. Yan, J.G. Zhu, and H.W. Lu, "Direct torque control of a surface-mounted permanent magnet synchronous motor based on accurate Modeling," *Proc. of Australasian Universities and Power Engineering Conf.*, Hobart, Australia., Sept. 2005, pp. 302-307.

[5] Y. Yan, J.G. Zhu, H.W. Lu, Y.G. Guo, and S.H. Wang, "Study of a PMSM model incorporating structural and saturation saliencies," *Proc. of 6th IEEE Int. Conf. on Power Electronics and Drive Systems*, Kuala Lumpur, Malaysia, Nov. 28 - Dec. 1, 2005, pp. 575-580.

[6] P. Cui, J.G. Zhu, Q.P. Ha, G.P. Hunter, and V.S. Ramsden, "Simulation of non-linear switched reluctance motor drive with PSIM," *Proc. of 5th Int. Conf. on Electrical Machines and Systems*, Shenyang, China, Aug. 2001, vol. 1, pp. 1061-1064.

[7] N. Matsui and T. Takeshita, "A novel starting method of sensorless salient-pole brushless motor," *Conference Record of the 1994 IEEE Industry Applications Society Annual Meeting*, Oct. 2-6, 1994, vol. 1, pp. 386–392.

[8] P.B. Schmidt, M.L. Gasperi, G. Ray, and A.H. Wijenayake, "Initial rotor angle detection of a nonsalient pole permanent magnet synchronous machine," *Conference Record of the 1997 IEEE Industry Applications Society Annual Meeting*, Oct. 5-9, 1997, Vol. 1, pp. 459-463.